Friction Pressure Loss in Microchannel Rarefied Gas Flows

Nevena Stevanović
Teaching and Research Assistant
University of Belgrade
Faculty of Mechanical Engineering

Gas flows through micro-channels are encountered in many applications of Micro-Electro-Mechanical Systems (MEMS) Dimensions of the MEMS are within μm *range, which means that rarefaction must be considered. It is common to use slip conditions at the wall and continuum equations for solving these problems. In this paper isothermal, compressible and subsonic gas flows through microchannels with slowly varying cross sections are analysed. In order to provide a higher accuracy, the second order boundary conditions are used. This approach requires the higher order momentum equation, i.e. the Burnett equation. Solutions are obtained for higher Reynolds number values when the inertia effect is important together with the rarefaction effect. For such flow conditions analytical relations for pressure and velocity fields are presented. Also, analytical expressions for the friction factor change along a microchannel with constant cross section and for the average friction factor are obtained. The derived relations show that the friction factor depends not only on the Reynolds number, but also on the Knudsen number.*

Keywords: *microchannel, slip flow, rarefaction, inertia, friction factor.*

1. INTRODUCTION

Two decades ago a production of very small devices began. These devices comprise both electrical and mechanical components, have a size between 1μm and 1mm and are called Micro-Electro-Mechanical Systems. They have found application in various fields of industry and medicine [1, 2, 3]. Accelerometers with a size of the order of microns are used for the activation of air bags in cars. Small pressure sensors are placed at the top of catheters that are used for the examination of blood vessels. Microactuators govern the electronic microscope in order to detect atoms. Micro heat exchangers are used for the cooling of electrical circuits. Micropumps are a part of inkjet printers. Micropumps and network of microchannels are applied in biomedical experiments for analyses of a drug deposition in the living tissue. One of the first examples of the phenomena of fluid flow in microchannels was encountered in the computer industry. The head of the Winchester hard disk is positioned at a distance of 50 nm above the rotating disk surface. The decrease of that distance leads to the increase of a disk capacity. NASA has encountered a need for a development of microsatellites. Their application increases a flexibility of a mission, and they can also be used as communication satellites in the Earth orbit. Movement and control of the microsatellites are achieved by micronozzles.

Received: May 2005, Accepted: July 2005.
Correspondence to: Nevena Stevanović
Faculty of Mechanical Engineering,
Kraljice Marije 16, 11120 Belgrade 35, Serbia and Montenegro
E-mail: nstevanovic@mas.bg.ac.yu

The flow of gases through microchannels of different shapes is present in the MEMS systems mentioned above. The first conclusion could be that there was no difference between the gas flow through the channels of ordinary dimensions and the microchannels. But, in the system of small dimensions, the surface effects are dominant [4]. The surface to volume ratio in machines with dimensions of 1 m is of the order of $1\ \mathrm{m}^{-1}$, while this ratio is $10^6\ \mathrm{m}^{-1}$ in the MEMS devices with characteristic length of 1 μm . This fact directly influences the transport of mass, momentum and energy at the interface of fluid and wall of a MEMS device. The application of the continuum models in the calculation of the fluid flow in channels of small dimensions is questionable, together with the application of the corresponding boundary conditions that a fluid in contact with wall has the same velocity as the wall surface due to the viscosity forces. Various effects must be taken into account in case of microchannel flows, such as gas rarefaction, slip conditions, thermal creeping and temperature jump at the wall.

The Knudsen number characterises the gas rarefaction. It is defined as the ratio of the mean free path λ and the characteristic length h: $Kn = \lambda / h$. The mean free path is proportional to the temperature and inversely proportional to the pressure. The effect of gas rarefaction occurs not only in devices that operate with low pressures and high temperatures, but also in devices with small dimensions (MEMS), since their characteristic dimensions are not negligible in comparison with the mean free path. The different Knudsen number regimes can be classified as: $Kn < 0.001$ - continuum flow, $0.001 < Kn < 0.1$ - slip

flow, $0.1 < Kn < 10$ - transitional flow and $Kn > 10$ - free molecular flow.

Gas microchannel flows in MEMS devices are mostly performed in the slip flow regime. It was observed by experiments that pressure distributions along microchannels are not linear. Also, higher mass flow rates were measured than the values predicted with the continuum theory. These suggested that continuum theory cannot be used any more in the slip flow regime. The deviation from continuum is taken into account through velocity slip and temperature jump boundary conditions that were first defined by Maxwell in 1879 and Smoluchowski in 1898

$$\tilde{u}_g - \tilde{u}_w = \frac{2-\sigma_v}{\sigma_v}\lambda\frac{\partial\tilde{u}}{\partial\tilde{n}}\bigg|_w + \frac{3}{4}\frac{\tilde{\mu}}{\tilde{\rho}\tilde{T}}\frac{\partial\tilde{T}}{\partial\tilde{s}}\bigg|_w, \quad (1)$$

$$\tilde{T}_g - \tilde{T}_w = \frac{2-\sigma_T}{\sigma_T}\left(\frac{2\gamma}{\gamma+1}\right)\frac{\lambda}{Pr}\frac{\partial\tilde{T}}{\partial\tilde{n}}\bigg|_w, \quad (2)$$

where $\tilde{u}_g$ and $\tilde{T}_g$ refer to the gas velocity and temperature at the wall, $\tilde{u}_w$ and $\tilde{T}_w$ are the velocity and temperature of the wall. Operators $\partial/\partial\tilde{n}$ and $\partial/\partial\tilde{s}$ denote the normal and tangential derivates at the surface respectively, σ_v and σ_T are accommodation coefficients of the solid surface, $\tilde{\mu}$, $\tilde{\rho}$, $\tilde{u}$, $\tilde{T}$ are dynamic viscosity, density, velocity and temperature respectively, γ is specific heat ratio and Pr is the Prandtl number. Sign $\sim$ denotes dimensional velocity, temperature, density, viscosity and coordinates.

Beskok and Karniadakis [5, 6, 7, 8] included a second order effect in boundary conditions leading to an increased accuracy

$$\tilde{u}_g - \tilde{u}_w = \frac{2-\sigma_v}{\sigma_v}\left[\lambda\frac{\partial\tilde{u}}{\partial\tilde{n}}\bigg|_w + \frac{\lambda^2}{2!}\frac{\partial^2\tilde{u}}{\partial\tilde{n}^2}\bigg|_w + \ldots\right] + \ldots, \quad (3)$$

$$\tilde{T}_g - \tilde{T}_w = = \frac{2-\sigma_T}{\sigma_T}\left(\frac{2\gamma}{\gamma+1}\right)\frac{1}{Pr}\left[\lambda\frac{\partial\tilde{T}}{\partial\tilde{n}}\bigg|_w + \frac{\lambda^2}{2!}\frac{\partial^2\tilde{T}}{\partial\tilde{n}^2}\bigg|_w + \ldots\right] \quad (4)$$

2. PROBLEM STATEMENT AND GOVERNING EQUATIONS

An isothermal, compressible and steady-state gas flow will be analysed and modelled for the low Mach number flow conditions in the microchannel with a slowly varying cross section, as shown in Fig. 1. The gas flow is driven by a pressure difference between the channel inlet and exit.

The stated problem is two-dimensional and could be described with the following mass and momentum conservation equations:

$$\frac{\partial(\tilde{\rho}\tilde{u})}{\partial\tilde{x}} + \frac{\partial(\tilde{\rho}\tilde{v})}{\partial\tilde{y}} = 0, \quad (5)$$

$$\frac{\partial(\tilde{\rho}\tilde{u}^2)}{\partial\tilde{x}} + \frac{\partial(\tilde{\rho}\tilde{u}\tilde{v})}{\partial\tilde{y}} = -\frac{\partial\tilde{p}}{\partial\tilde{x}} + \frac{\partial\tilde{\tau}_{xx}}{\partial\tilde{x}} + \frac{\partial\tilde{\tau}_{yx}}{\partial\tilde{y}}, \quad (6)$$

$$\frac{\partial(\tilde{\rho}\tilde{u}\tilde{v})}{\partial\tilde{x}} + \frac{\partial(\tilde{\rho}\tilde{v})}{\partial\tilde{y}} = -\frac{\partial\tilde{p}}{\partial\tilde{y}} + \frac{\partial\tilde{\tau}}{\partial\tilde{x}} + \frac{\partial\tilde{\tau}}{\partial\tilde{y}}, \quad (7)$$

where $\tilde{\rho}$ is density, $\tilde{p}$ is pressure, $\tilde{u}$ and $\tilde{v}$ are velocity components. Viscous stresses are denoted with $\tilde{\tau}_{ji}$. The equation of the ideal gas $\tilde{p} = \tilde{\rho}R\tilde{T}$ is added to the above set.

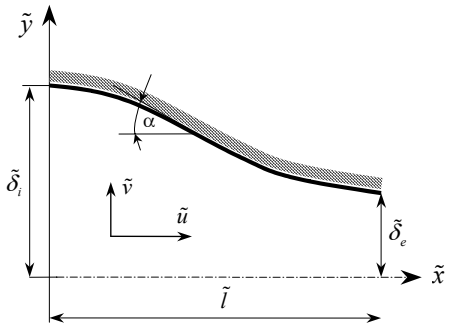

Figure 1. Microchannel with the slowly varying cross section.

In this paper the second order boundary conditions defined by Beskok and Karniadakis [5, 6, 7, 8] are used in order to obtain the higher accuracy. According to this approach, the second order equations for the viscous stresses are applied in the momentum equations. These are Burnett equations [6, 9, 10, 11].

The system of basic equations is transformed into a non-dimensional form by the introduction of the following scales: $\tilde{\delta}_e$ for all lengths, the exit average velocity $\tilde{u}_e$ for all velocities, the exit pressure $\tilde{p}_e$ and the exit density $\tilde{\rho}_e$ at the axes in the outlet cross section for pressure and density, respectively. Non-dimensional velocity, pressure, density, temperature and coordinates will be denoted by u, v, p, ρ, T, x, y. The assumption of low Mach number flow conditions enables the definition of the small parameter $\varepsilon = \gamma Me^2/Re$, where γ is the ratio of specific heats, Me is the referent Mach number value defined as $Me = \tilde{u}_e/\sqrt{\gamma\,\tilde{p}_e/\tilde{\rho}_e}$ and Re is the referent Reynolds number value $Re = \tilde{\rho}_e\tilde{u}_e\tilde{\delta}_e/\tilde{\mu}$. Dynamic viscosity $\tilde{\mu}$ is constant. From the definition of the small parameter ε, the relation $\varepsilon = \tilde{\mu}\dot{m}/2\tilde{\rho}_e\tilde{p}_e\tilde{\delta}_e^2$ follows, where $\dot{m} = 2\tilde{\rho}_e\tilde{u}_e\tilde{\delta}_e$ represents channel mass flow rate per unit width. The assumption of the slowly varying channel cross section ($\alpha \approx \varepsilon << 1$, α is channel wall inclination, Fig. 1.) implies that all flow parameters change vary slowly in the x - axes direction, which is explicitly expressed by the introduction of the slow coordinate $\xi = \varepsilon x$. Also, the crosswise velocity component v is much smaller than the streamwise component u, which leads to the following relations $v(x,y) = \varepsilon V(\xi, y)$, $V = O(1)$. Hence, the obtained

continuity and momentum equations and the equation of state have the following non-dimensional form:

$$\partial(pu)/\partial\xi + \partial(pV)/\partial y = 0\,, \tag{8}$$

$$\gamma Me^2 p\left(u\frac{\partial u}{\partial\xi} + V\frac{\partial u}{\partial y}\right) = -\frac{\partial p}{\partial\xi} + \frac{\partial^2 u}{\partial y^2} + O\left(\varepsilon^2\right), \tag{9}$$

$$\frac{\partial p}{\partial y} = O\left(\varepsilon^2\right), \tag{10}$$

$$p = \rho\,. \tag{11}$$

Obtained Eqs. (9) and (10) are the Burnett equations, which have the same form as the Navier-Stokes equations under the stated flow conditions. Here, presented analytical derivation shows that the Navier-Stokes equations can describe the flow conditions with larger deviations from the continuum if the values of the Mach and Reynolds numbers enable a definition of the small parameter ε. This conclusion confirms the usage of the Navier-Stokes equations with the second order boundary conditions for a slip flow regime under conditions defined in this paper.

Since the mean free path of molecules under isothermal flow conditions is inversely proportional to pressure, the local Knudsen number ($Kn = \lambda/\tilde{\delta}_e$) would be expressed as Ke/p [12], where Ke is the referent Knudsen number $Ke = \sqrt{\frac{\pi\gamma}{2}}\frac{Me}{Re}$ ($Ke = \lambda_e/\tilde{\delta}_e$) and p is the non-dimensional pressure in any channel cross section. By using already defined scales for length and velocity, Beskok and Karniadakis boundary condition can be written in non-dimensional form:

$$y = \delta(\xi): u\text{-}u_w = \frac{2-\sigma_v}{\sigma_v}\left[-\frac{Ke}{p}\frac{\partial u}{\partial y} + \frac{Ke^2}{2p^2}\frac{\partial^2 u}{\partial y^2} + O\left(Ke^3\right)\right],$$
$$V = u\frac{\mathrm{d}\delta}{\mathrm{d}\xi}\,. \tag{12}$$

Also, symmetry conditions at the channel axes will be used. In non-dimensional form they are

$$y = 0: \quad \partial u/\partial y = \partial^3 u/\partial y^3 = \ldots = 0, \quad V = 0\,. \tag{13}$$

For low Mach number values the following relation holds $\gamma Me^2 = \beta\varepsilon^m$, $\beta = O(1)$, as well as $Ke = \eta\varepsilon^n$, $\eta = O(1)$ for low Knudsen number values. Parameter ε, Me and Ke numbers are dependant on mass flow rate, which leads to the conclusion that parameters β and η are also function of $\dot{m}$. The non-dimensional flow channel length is defined as $\xi_L = \varepsilon\left(\tilde{l}/\tilde{\delta}_e\right)$. Since the small parameter ε contains the mass flow rate, it can be concluded that the non-dimensional channel length ξ_L is proportional to the mass flow rate. Further, it can be concluded that parameter β is proportional to $\dot{m}^{2\text{-}m}$ and parameter η is proportional to $\dot{m}^{-n}$. They can be written as

$$\beta = M\xi_L^{\,2-m}\,,$$

where

$$M = \frac{\tilde{p}_e\tilde{\delta}_e^{\,2}\tilde{\rho}_e}{\tilde{\mu}^2}\left(\frac{\tilde{\delta}_e}{\tilde{l}}\right)^{2-m} = O(1)$$

and

$$\eta = N\xi_L^{\,-n}\,,$$

where

$$N = \sqrt{\frac{\pi}{2}}\frac{\tilde{\mu}}{\tilde{\delta}_e\tilde{\rho}_e\sqrt{R\tilde{T}}}\left(\frac{\tilde{\delta}_e}{\tilde{l}}\right)^{-n} = O(1)\,.$$

Since, only the Mach and Reynolds numbers are independent of each other, there is a relation between m and n, as well as between parameters β and η, i.e. M and N: $2n + m = 2$, $\eta = \sqrt{\pi/2\beta}$ and $N = \sqrt{\pi/2M}$. For low Mach and Knudsen number flows, m and n values must be positive and within the following ranges $0<m<2$ and $0<n<1$. In these ranges two characteristic cases are analysed:

1. $1<m<2 \Rightarrow 0<n<1/2$ when $Re \ll 1$. Chosen values of the parameters m and n, which represent the range of low Reynolds numbers are: m=3/2 and $n = 1/4$, which implies that $Re = \beta\varepsilon^{1/2}$, $\gamma Me^2 = \beta\varepsilon^{3/2}$ and $Ke = \eta\varepsilon^{1/4}$.
2. $0<m<1 \Rightarrow 1/2<n<1$ for $Re \gg 1$. Chosen values of the parameters m and n, which represent the range of moderately high Reynolds number are: m=n=2/3, which implies $Re = \beta\varepsilon^{-1/3}$, $\gamma Me^2 = \beta\varepsilon^{2/3}$ and $Ke = \eta\varepsilon^{2/3}$.

In this paper solutions for $Re \gg 1$ are obtained. The aim was to take into account the inertia effect together with the rarefaction. From momentum equation (9) and boundary condition Eq. (12) follows that a relation between Mach and Knudsen number must be satisfied: $\gamma Me^2 = O(Kn)$. If we write the Much number as $Me^2 = O\left(\varepsilon^q\right)$, the relation requires that $Ke = O\left(\varepsilon^q\right)$, and $|q| < 1$. However, if the reference Reynolds number is eliminated between our assumption $Me^2/Re = O(\varepsilon)$ and the relation $Ke = O(Me/Re)$, another relation between Me and Ke is obtained $MeKe = O(\varepsilon)$, which leads to the single value for q: $q = 2/3$. Thus, our theory holds for $Ke = O\left(\varepsilon^{2/3}\right)$ and $\gamma Me^2 = O\left(\varepsilon^{2/3}\right)$, which means that $m = 2/3$ and $n = 2/3$. Now, assumptions for Reynolds, Much and Knudsen numbers are $Re = \beta\varepsilon^{-1/3}$, $\gamma Me^2 = \beta\varepsilon^{2/3}$ and $Ke = \eta\varepsilon^{2/3}$.

All the dependant variables from Eqs. (8)-(11), i.e. pressure and velocity $F = F(u,v,p)$, are presented in the form of the perturbation series

$$F = F_0 + \varepsilon^{2/3} F_{2/3}, \tag{14}$$

where F_0 is the solution for flow with no-slip boundary conditions, and $F_{2/3}$ is the correction of physical parameters due to the slip effects on the wall and the inertia effect. The system of equations for two approximations is obtained with the standard method under the corresponding boundary conditions.

It seems that three flow parameters u, V, p can not be determined from two equations (continuity and momentum conservation equations in x direction). But, the number of boundary conditions is higher by one than the number of unknown parameters, and the problem is mathematically correctly defined. The solutions are obtained with the similar method for every approximation. The expression for the streamwise velocity is derived from the momentum equation in x-direction, by assuming that the pressure is known and with the application of appropriate boundary conditions. Crosswise velocity component $V(\xi, y)$ is derived from the equation of continuity (8). Integration of the continuity equation in the range from $y = 0$ to $y = \delta$ gives

$$\int_0^\delta pu\, dy = 1 \text{, or}$$

$$\int_0^\delta p_0 u_0 dy = 1 \quad \text{and} \quad \int_0^\delta (p_0 u_{2/3} + p_{2/3} u_0) \mathrm{d}y = 0 . \tag{15}$$

Their solution provides the pressure differential equation. Defining streamwise coordinate as $X = \xi/\xi_L$, equations for velocity and pressure for the first two approximations have the following form:
-the first approximation:

$$u_0 = -\frac{p_0' \delta^2}{2\xi_L}\left(1 - \frac{y^2}{\delta^2}\right), \tag{16}$$

$$V_0 = -\frac{p_0' \delta \delta'}{2{\xi_L}^2} y\left(1 - \frac{y^2}{\delta^2}\right), \tag{17}$$

$$p_0 p_0' = -3\xi_L / \delta^3 ; \tag{18}$$

-the second approximation:

$$u_{2/3} = \frac{\delta^2}{2}\left[\left(B - \frac{p_{2/3}'}{\xi_L}\right)\left(1 - \frac{y^2}{\delta^2}\right) - \frac{B}{3}\left(1 - \frac{y^4}{\delta^4}\right) + \frac{B}{15}\left(1 - \frac{y^6}{\delta^6}\right)\right] - \frac{2 - \sigma_v}{\sigma_v}\frac{\eta \delta p_0'}{\xi_L p_0}, \tag{19}$$

where $B = 9\beta(p_0\delta)' / \left(4\xi_L {p_0}^2 \delta^3\right)$,

$$\left(p_0 p_{2/3}\right)' = -\frac{2 - \sigma_v}{\sigma_v}\frac{3\eta p_0'}{\delta} + \frac{54}{35}\beta\frac{(p_0\delta)'}{p_0 \delta^3} \tag{20}$$

while prime denotes $\mathrm{d}/\mathrm{d}X$, and δ is the function for the channel cross section dependence on X.

For the known geometry of the channel and the pressure at the outlet, which are completely comprised within the first approximation $(X = 1,\ p = p_0 = 1)$, solutions for pressure and velocity fields in the whole channel will be obtained. Ratio of parameters β and η in the case analysed in this paper can be expressed as $\beta/\eta = \gamma Me^2/Ke$ i.e. $\beta/\eta = 2KeRe^2/\pi$.

3. FRICTION FACTOR IN MICROCHANNEL FLOWS BETWEEN PARALLEL PLATES

For channel with constant cross section $\delta(X) = 1$, the expression for the pressure change $p = p_0 + \varepsilon^{2/3} p_{2/3}$ is obtained in the following form:

$$p = p_0 + 3Ke\frac{2 - \sigma_v}{\sigma_v}\left(\frac{1}{p_0} - 1\right) + \frac{108}{35}\frac{Ke^2 Re^2}{\pi}\frac{\ln p_0}{p_0} \tag{21}$$

where p_0 is the solution for the first approximation

$$p_0 = \sqrt{1 + 6\xi_L (1 - X)} . \tag{22}$$

The second term on the r.h.s. in Eq. (21) is due to rarefaction, and the third term shows the influence of inertia. The comparison between them leads to the conclusion that the inertia is dominant when

$$Re > \sqrt{\frac{2 - \sigma_v}{\sigma_v}\frac{35\pi}{36Ke}\frac{|1 - p_0|}{\ln p_0}} . \tag{23}$$

Now, the friction factor ($f = \tilde{\tau}_w / \frac{1}{2}\tilde{\rho}\bar{\tilde{u}}^2$) for rarefaction gas flow can be defined. According to the conclusion that the Burnet equations have the same form as the Navier Stokes equations within the approximations made in this paper, the shear stress on the wall surface is $\tilde{\tau}_w = -\left(\tilde{\mu}\frac{\partial \tilde{u}}{\partial \tilde{y}}\right)_{\tilde{y}=\tilde{\delta}}$, and $\bar{u}$ is the average cross section velocity. In this paper a change of the friction factor along the microchannel with the constant cross section will be analysed. Using the same scales for velocity, pressure, density and length, and including the fact that for isothermal flow conditions the dimensionless average velocity is inversely proportional to the dimensionless pressure, the expression for the friction factor in non-dimensional form becomes:

$$f = -\frac{2p}{Re}\left(\frac{\partial u}{\partial y}\right)_{y=1} . \tag{24}$$

Substituting equations for velocity (16) and (19) and pressure Eqs. (21) and (22) for the flow between parallel plates, into Eq. (24), the following expression is obtained

$$f = -\frac{2p}{Re \cdot \xi_L}\left(p' - \frac{12}{5\pi} Ke^2 Re^2 \frac{p_0'}{p_0^2} \right). \quad (25)$$

This expression shows the friction factor dependence upon Reynolds and Knudsen number. The friction factor for compressible flow without slip is obtained as

$$f_{comp(Ke=0)} = -\frac{2p_0 p_0'}{Re\xi_L}. \quad (26)$$

Introducing Eq. (18) in (25) the following equation is derived

$$f_{comp(Ke=0)} = \frac{6}{Re}. \quad (27)$$

Equation (27) shows that the friction factor is constant along the channel and it has the same form as in case of the incompressible flow between parallel plates.

In order to design microdevices properly, it is necessary to know the average friction factor in microchannels $\overline{f} = \int_0^1 f \, dX$. Substituting Eq. (25) in this integral, the following expression for the average friction factor is obtained

$$\overline{f} = \left[P^2 - 1 - \frac{72}{15\pi} Ke^2 Re^2 \ln P_0 + \right.$$
$$+ \frac{36}{5\pi} \frac{2 - \sigma_v}{\sigma_v} Ke^3 Re^2 \left(\frac{P_0 - 1}{P_0} \right)^2 -$$
$$\left. - \frac{648}{175\pi^2} Ke^4 Re^4 \left(1 - \frac{2\ln P_0 + 1}{P_0^2} \right) \right] \Big/ Re \cdot \xi_L \quad (28)$$

The ratio of inlet to outlet pressure for the slip flow condition is P, and for the no-slip condition is P_0. Both pressure ratios are obtained for the same mass flow, geometry and conditions at the exit cross section. P and P_0 follow from Eqs. (21) and (22) when $X = 0$. As it could be expected, the average friction factor depends on the Reynolds and Knudsen number and parameter $\xi_L = f(\varepsilon, l/\delta)$.

The average normalised friction factor $\overline{C^*} = \left(\overline{f} \cdot Re\right) / \left(f_{Ke=0} \cdot Re\right)$ based on the second order model is obtained from Eqs. (27) and (28) as

$$\overline{C^*} = \left[P^2 - 1 - \frac{72}{15\pi} Ke^2 Re^2 \ln P_0 + \right.$$
$$+ \frac{36}{5\pi} \frac{2 - \sigma_v}{\sigma_v} Ke^3 Re^2 \left(\frac{P_0 - 1}{P_0} \right)^2 -$$
$$\left. \frac{648}{175\pi^2} Ke^4 Re^4 \left(1 - \frac{2\ln P_0 + 1}{P_0^2} \right) \right] \Big/ 6\xi_L. \quad (29)$$

Obtained expression represents a deviation of the friction factor for slip flow from the friction factor for no-slip conditions.

4. RESULTS AND DISCUSSION

Figure 2 shows the friction factor changes along the microchannel for different *Re* and *Ke* numbers and under flow conditions that satisfy $\xi = 1$. The results presented with the full lines are calculated with Eq. (25), which is derived by taking into account the inertia effects (the complete model solution), while the dashed line represents a solution obtained with the simplified model that does not comprise the influence of inertia forces on the friction factor. The simplified model solution is given with the following equation, obtained by neglecting the second term in the parentheses of Eq. (25) and the last term on the r.h.s. of Eq. (21)

$$f = -2\frac{pp'}{Re\,\xi_L}. \quad (30)$$

The complete model solutions (full lines in Fig. 2) show that for low Knudsen number values the friction factor decreases along the microchannel, and for higher Knudsen numbers (for $Re = 10$ and $Ke = 0.1$, and $Re = 20$ and $Ke = 0.03$ and 0.05 in Fig. 2) the friction factor increases in the end part of the microchannel due to the inertia effect. This influence of inertia is clearly demonstrated by comparison with the dashed line, which is obtained by simplified model that neglects the inertia effect. Figure 2b) shows that the inertia effect leads to the increase of the friction factor, whose values are even higher than in case of no slip flow (denoted with $Ke = 0$).

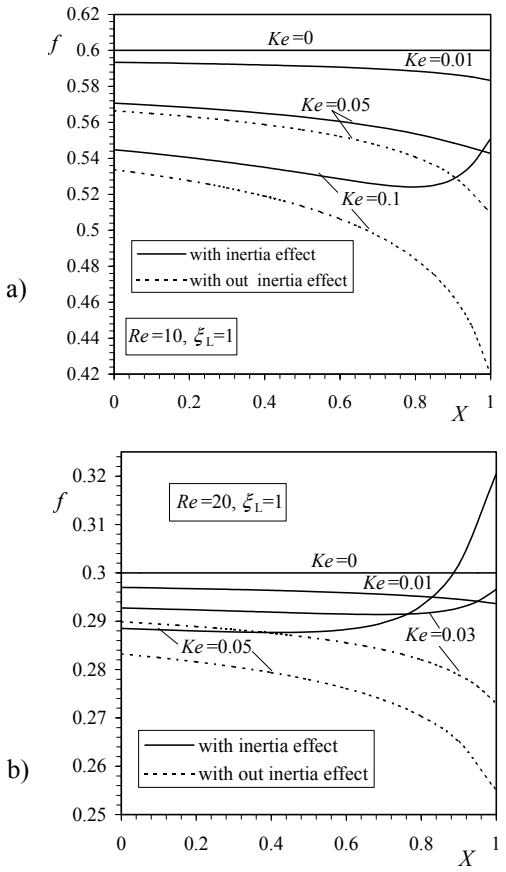

Figure 2. Friction factor change along microchannel for ξ_L=1: a) *Re*=10, b) *Re*=20.

In Fig. 3 the average friction factor dependence on *Re* and *Ke* numbers is shown. The average friction factor is calculated with Eq. (28) for known flow conditions. In spite of the phenomenon that the local friction factor values in some cases increase in the exit part of the microchannel (due to the inertia effect), and even reaches values higher than in case of no slip conditions, here obtained average values of the friction factor are lower than the values of no slip flow conditions.

In [13] the local normalised friction factor is derived on the basis of the first order slip model in the form $C^* = 1/(1+3Kn)$. The first order model does not take

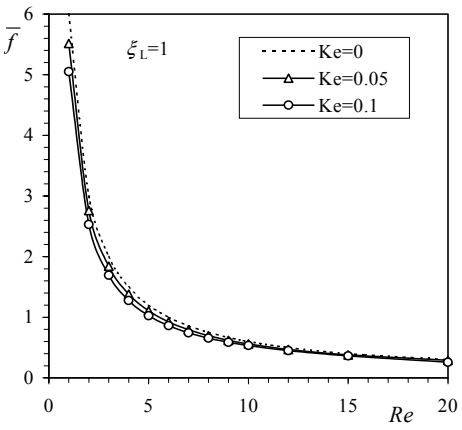

Figure 3. Average friction factor for ξ_L =1.

into account the inertia effect and the second order slip conditions. In the work presented herein the relation for local normalised friction factor leads from Eqs. (25) and (27)

$$C^* = -\frac{p}{3\cdot\xi_L}\left(p' - \frac{12}{5\pi}Ke^2Re^2\frac{p_0'}{p_0^2}\right). \qquad (31)$$

This relation is obtained as a result of the second order theory, and, as described, it also includes the inertia effect. If the inertia terms from Eq. (31) are neglected, it becomes the same as the above mentioned equation obtained from the first order theory.

In Fig. 4 the normalised friction factor C^* dependence on *Re* and *Ke* number is shown. Results presented in this figure are obtained for a typical value $\xi_L = 1$. Presented values of C^* are lower than 1 for slip flows (curves for *Ke*>0). Parameter C^* decreases with the increase of *Ke* number, which means that the deviation from no slip condition is higher for a higher value of the Knudsen number. The appearance of the maximum of the curve for *Ke* = 0.1 is the result of the inertia effect included in the work presented herein.

In order to compare results of the work presented herein with available experimental data, the friction factor calculation is performed with the value of dimensionless parameter $\xi_L = 0.01$, because it is estimated that the experimental value of parameter ξ_L is about $O(10^{-2})$.

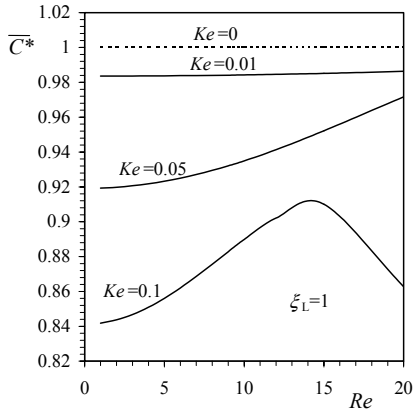

Figure 4. Normalised friction factor for ξ_L =1.

Figure 5 shows a comparison of analytical results calculated with the work presented herein and the correlation derived from the experimental data [14] in the following form

$$\overline{f} = 24/(Re(1+4.7Ke)) \qquad (32)$$

where *Re* is the Reynolds number based on the hydraulic diameter of the channel ($Re = \tilde{\rho}\overline{u}\tilde{D}_h/\tilde{\mu}$) and *Ke* is the Knudsen number defined as $Ke = \lambda/2\tilde{\delta}$. The acceptable agreement is shown. Analytical results show a dependence of the average friction factor on the Reynolds number and the rarefaction effect expressed with the Knudsen number. At lower Reynolds numbers the average friction factor decreases with the *Ke* increase. The opposite holds for higher Reynolds numbers due to the inertia effect.

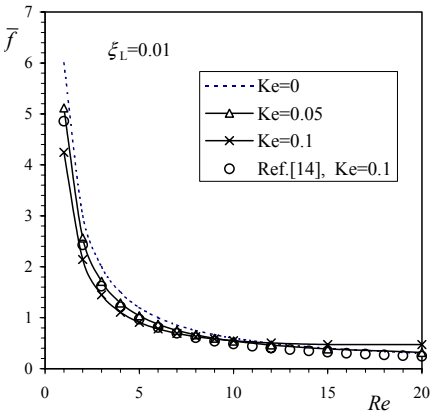

Figure 5. Average friction factor for ξ_L =0.01.

The local values of the friction factor along the dimensionless microchannel length are shown in Fig. 6 for two Reynolds numbers and several Knudsen numbers. The friction factor is practically constant along the channel, but its value strongly depends on the *Ke* and *Re* numbers. The increase of the Knudsen number up to a certain value leads to the friction factor decrease, while further *Ke* number increase leads to the friction factor increase (the friction factor for *Ke*=0.05 and *Re*=20 is even higher than the value for the no slip conditions presented with line *Ke*=0 in Fig. 6b). This behaviour is caused by the inertia effect, and it is

equivalent to the behaviour shown in Fig. 2. As explained, the influence of inertia is manifested at the exit part of the channel in Fig. 2 (obtained under dimensionless parameter $\xi_L = 1$), but in Fig. 6 the influence of inertia is felt along the whole channel due to the lower value $\xi_L = 0.01$.

The influence of inertia shown in Figs. 5 and 6 is also demonstrated in Fig. 7 where dependence of the normalised friction factor on the Reynolds number is depicted.

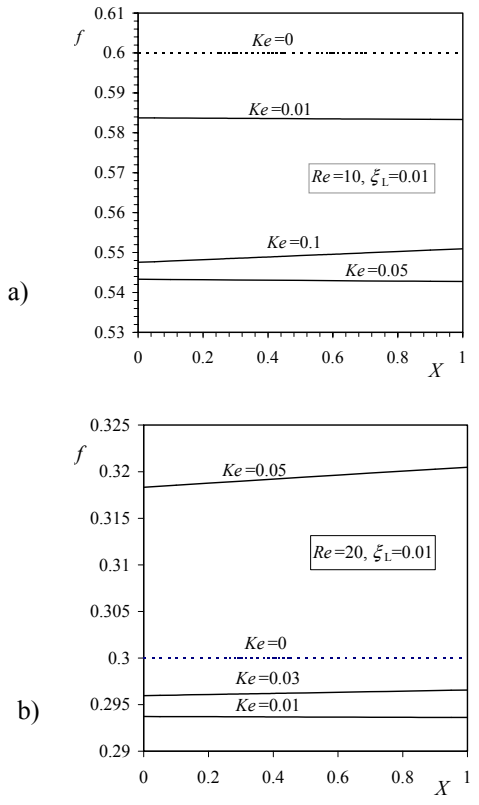

Figure 6. Friction factor change along microchannel for ξ_L =0.01: a) *Re*=10, b) *Re*=20.

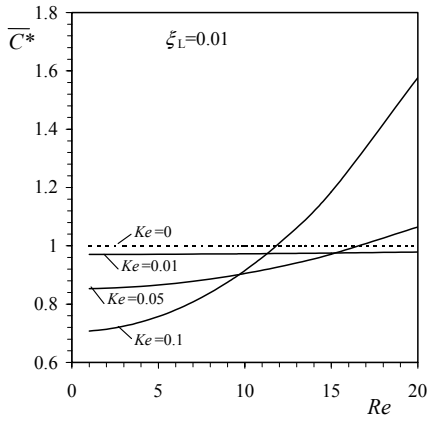

Figure 7. Normalised friction factor for ξ_L =0.01.

The classical one-dimensional theory for isothermal compressible gas flow between parallel plates gives

$$\overline{f}\frac{(\tilde{x}_2-\tilde{x}_1)}{\tilde{\delta}} = \psi(Ma_2) - \psi(Ma_1) \qquad (33)$$

Here $\psi(Ma) = -\frac{1}{\gamma Ma^2} - \ln Ma^2$, where subscript 1 refers to the Mach number in the cross section at distance $\tilde{x}_1$ from the inlet cross section and subscript 2 refers to the channel exit ($Ma_2 = Me$). For isothermal flow conditions, the Mach number along the microchannel can be defined as $Ma_1 = Me/p$. Then equation (30) can be written in the following form

$$\overline{f}\frac{(\tilde{x}_2-\tilde{x}_1)}{\tilde{\delta}} = \frac{p^2-1}{\gamma Me^2} - \ln p^2 . \qquad (34)$$

According to the two-dimensional theory already described in this paper, the following relation holds $\frac{\tilde{x}}{\tilde{\delta}} = \xi_L \frac{X}{\varepsilon}$. Employing this relation and well-known relation between *Me*, *Re* and *Ke* numbers in Eq. (34) it follows:

$$\overline{f}\, Re\, \xi_L \Delta X = p^2 - 1 - \frac{4Ke^2 Re^2}{\pi}\ln p , \qquad (35)$$

where ΔX is the distance from the exit expressed with *X*.

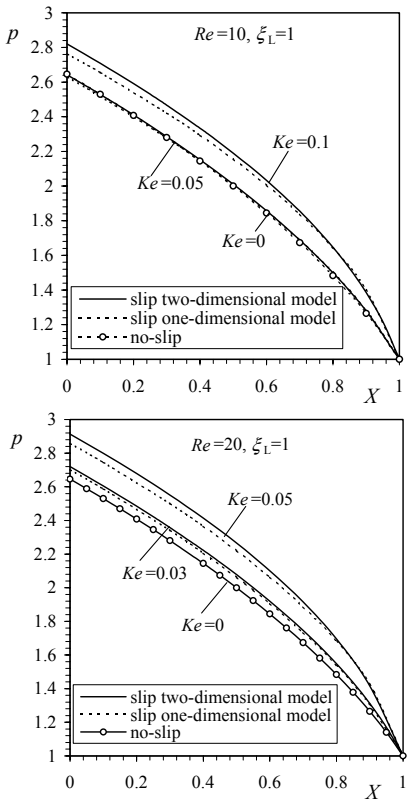

Figure 8. Pressure distribution in microchannel for ξ_L =1.

For known flow conditions, the average friction factor can be calculated from Eq. (28), and then pressure distribution from two-dimensional Eq. (21) and one-dimensional Eq. (35) theory. In Figs. 8 and 9 a comparison of these two theories is presented. Differences between results of the pressure distribution along the channel obtained with these two theories are not large. For higher rarefaction effect (higher *Kn* number value) the difference is more pronounced.

The pressure distribution for the compressible flow is not linear. This effect is more exaggerated in Fig. 8.

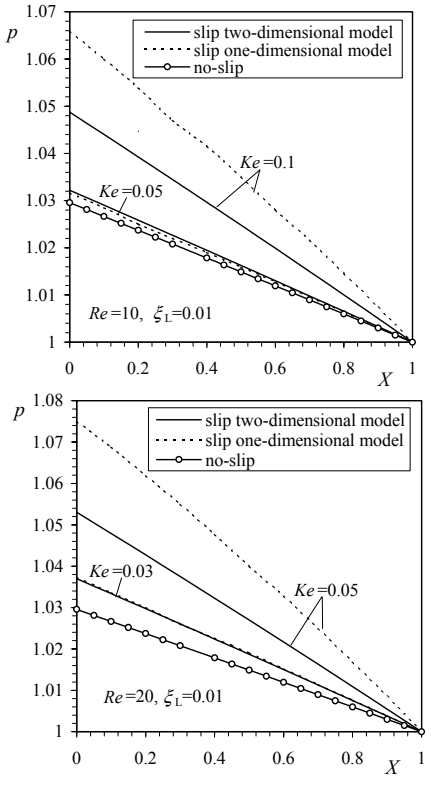

Figure 9. Pressure distribution in microchannel for ξ_L =0.01.

5. CONCLUSION

Two-dimensional model for the isothermal compressible subsonic gas flow in microchannels are presented in this paper. Analytical solutions for the pressure and friction factor change along microchannels are obtained. Influences of both rarefaction and inertia effects are analysed.

It is concluded that the rarefaction effect causes a lower pressure in the microchannel than in case when the rarefaction is neglected. The inertia has the opposite effect, leading to the pressure increase, and in some cases the pressure becomes even higher than in the no-slip flow.

The same holds for the friction factor. If the rarefaction were the only analysed effect, the friction factor would be always lower than in the no-slip conditions. But the influence of inertia makes that in some cases the friction factor becomes higher than in no-slip flow. Analytical results show that the friction factor depends not only on the Reynolds number, but also on the Knudsen number.

REFERENCES

[1] Karniadakis, G. and Beskok, A., *Micro Flows*, Springer-Verlag, New York, 2002.

[2] Gad-El-Hak, M.: The Fluid Mechanics of Microdevices-The Freeman Scholar Lecture, J. Fluids Engineering, Vol. 121, pp. 5—33. 1999.

[3] Gad-El-Hak, M., *The MEMS Handbook*, CRC Press, 2002.

[4] Trimmer, W. and Stroud, H.R.: Scaling of Micromechanical Devices, *The MEMS Handbook*, Editor Gad-el-Hak, M., CRC Press, 2002.

[5] Beskok, A and Karniadakis, G.: Simulation of heat and momentum transfer in complex micro-geometries, J. of Thermophysics and Heat Transfer, Vol. 8, No. 4, pp. 647-655. 1994.

[6] Beskok, A and Karniadakis, G.: A Model for Flows in Channels, Pipes and Ducts at Micro and Nano Scales, Microscale Thermophys. Eng., Vol. 3, pp. 43-77. 1999.

[7] Beskok, A., Karniadakis, G. and Trimmer, W.: Rarefaction and Compressibility Effects in Gas Microflows, J. Fluids Eng., Vol.118, No. 3, pp. 448-456. 1996.

[8] Beskok, A.: Validation of a New Velocity-Slip Model for Separated Gas Microflows, Numerical Heat Transfer, Vol. 40, pp. 451-471. 2001.

[9] Vinsenti, G.W. and Kruger, H.C., *Introduction to Physical Gas Dynamics*, R.E. Krieger Publishing Company, Malabar, Florida, 1986.

[10] Schaaf, A.S.: Mechanics of Rarefied Gases, *In Encyclopedia of Physics*, Springer-Verlag-Berlin, Vol. VIII/2, pp. 591-625. 1963.

[11] Schaaf, A.S. and Chambre, A.P. : Flow of Rarefied Gases, *In Fundamentals of Gas Dynamics*, Editor Emmons, W.H., Princeton University Press, Princeton. 1958.

[12] Stevanovic, N.: A theoretical contribution to the rarefied gas flow in microchannels, PhD thesis, Faculty of Mechanical Engineering, Belgrade, 2004.

[13] Araki, T., Kim, M.S., Iwai, H. and Suzuki, K.: An experimental investigation of gaseous flow characteristics in microchannels, Microscale Thermophys. Eng., Vol. 6, pp. 117-130. 2002.

[14] Hsieh, S.S., Tsai, H.H., Lin, C.L., Huang, C.F. and Chien, C.M.: Gas flow in a long microchannel, Int. J Heat Mass Transfer, Vol 47, pp. 3877-3887. 2004.

ПАД ПРИТИСКА УСЛЕД ТРЕЊА ПРИ СТРУЈАЊУ РАЗРЕЂЕНОГ ГАСА У МИКРОКАНАЛИМА

Невена Стевановић

Струјање гаса кроз микроканале присутно је у микро електро механичким системима (MEMC). Димензије микроканала су реда величине μm, па дужина слободног пута молекула није занемарљиво мала. Ефекат разређености долази до изражаја, па је потребно узети у обзир граничне услове клизања на зиду. У овом раду добијена су решења за дводимензијско, изотермско, стишљиво струјање гаса кроз микроканале споро променљивог попречног пресека, при веома малим вредностима Mach-овог броја. Коришћени су гранични услови клизања другог реда, што је условило коришћење и једначина количине кретања другог реда, тј. Burnett-ових једначина. Показало се да се за поменуте услове струјања оне своде на Navier-Stokes-ове. У раду је приказано аналитичко решење за случајеве струјања гаса када је вредност Reynolds-овог броја већа, па осим разређености до изражаја долази и утицај инерције. За такве услове струјања добијена су решења за поље притиска и брзине, као и аналитички изрази за одређивање фактора трења дуж канала и његове средње вредности. Из њих се види да при струјању разређеног гаса фактор трења зависи и од Reynolds-овог и од Knudsen-овог броја.